A new method for screening glutathione reductase inhibitors using square wave voltammetry

Article *in* Analytical Methods · May 2015

DOI: 10.1039/C5AY00347D

CITATIONS
4

READS
220

5 authors, including:

M. S. Karacan
Gazi University
22 PUBLICATIONS **262** CITATIONS
SEE PROFILE

Turgay Tunc
Ahi Evran Üniversitesi
16 PUBLICATIONS **66** CITATIONS
SEE PROFILE

Serhat Mamaş
Gazi University
13 PUBLICATIONS **177** CITATIONS
SEE PROFILE

Nurcan Karacan
Gazi University
58 PUBLICATIONS **1,081** CITATIONS
SEE PROFILE

Analytical Methods

PAPER

View Article Online
View Journal | View Issue

Cite this: *Anal. Methods*, 2015, **7**, 5142

A new method for screening glutathione reductase inhibitors using square wave voltammetry

Mehmet Sayım Karacan,*[a] Turgay Tunç,[b] Hatice Oruç,[a] Serhat Mamaş[a] and Nurcan Karacan[a]

Received 6th February 2015
Accepted 15th May 2015

DOI: 10.1039/c5ay00347d

www.rsc.org/methods

A square wave voltammetric method was developed for the detection of glutathione reductase (GR) activity. The method is based upon the direct determination of glutathione (GSH) produced by nicotinamide adenine dinucleotide phosphate (NADPH)-dependent reduction of glutathione disulfide (GSSG). Enzyme activity was represented by an increase in steady-state reduction current of GSH and this current was monitored voltammetrically. At the optimized working condition, reduction potential of GSH was found at −0.44 V with a hanging mercury drop electrode *versus* an Ag/AgCl electrode. The reduction current was directly proportional to GSH concentration in the range 2.63–800 μM with a lower detection limit of 0.79 μM and lower quantification limit of 2.63 μM. Inhibitory activities of four antimony(III) compounds were determined by this method, and obtained IC_{50} values were compared with previous data. In addition, an electrochemical study of these compounds showed that their reductions have an EC mechanism; the current is diffusion controlled, and $E_{p/2}$ values are proportional to inhibitor activity.

Introduction

Glutathione reductase, a flavoprotein, is an important enzyme in cells and plays a critical role in maintenance of redox states of intracellular species, cleansing of free radicals and reactive oxygen species, intracellular signal transduction and gene regulation[1–4] by maintaining a high ratio of GSH/GSSG.[5] Under normal conditions, glutathione exists mainly in the reduced form (GSH); nonetheless, it may be quickly oxidized to GSSG when reacting to oxidative stress in a cell. However, glutathione reductase reduces GSSG to GSH with NADPH and maintains the intracellular mol ratio of GSH/GSSG above 99%.

$$GSSG + NADPH + H^+ \rightarrow 2\,GSH + NADP^+$$

Owing to the key function of GSH in numerous cellular processes, GSH levels and the GSH/GSSG ratio have been related to numerous human illnesses, for instance Alzheimer, AIDS, diabetes, alcoholic liver, cardiovascular disease and cancer.[6–14] GSH is also utilized for detoxification of heme[15–17] and the increase in intracellular GSH quantity was responsible for the development of Chloroquine resistance.[18,19] On the other hand, glutathione reductase inhibitors are found to possess antimalarial and anticancer activity.[20] Therefore, the sensitivity of any method used in the determination of glutathione reductase activity is important. The classic methods,[21] still widely used for the determination of glutathione reductase activity, are based on spectrometrically measuring the concentration of NADPH at 340 nm. However, this method may prove to be inadequate due to interferences by absorption peaks of inhibitors. For this reason, new methods and sensors such as high-performance liquid chromatography with electrochemical detection,[22] fluorometric assay,[23] amperometric sensors,[24] fluorescent probes[25] and quantum dots[26] have been developed to detect glutathione reductase activity.

Many other methods have been developed and improved for determining GSH and GSSG content with different samples. These include chromatography,[27–31] LCMS/MS,[32,33] capillary electrophoresis/electrochemiluminescence,[34] HPLC/UV,[35] luminescence,[36] and voltammetric[37–39] techniques.

Corrêa-da-Silva *et al.*[38] were the first to use a hanging mercury electrode to quantify GSH in biological samples buffered with phosphates (pH 7.5) and their work inspired several other attempts. In this context electrochemical methods based on modified electrodes[39–41] and a modified glassy carbon electrode[38] were reported.

In this study, we use a square wave voltammetric (SWV) method for the first time to measure *in vitro* the GR inhibitory activity in order to develop a simple and low-cost system. With the aid of this method, IC_{50} values of four different antimony(III) complexes were determined and the results were compared with those obtained spectrophotometrically.[42] The electrochemical properties of the complexes were also investigated by using voltammetric methods.

[a]*Gazi University, Science Faculty, Chemistry Department, 06500, Ankara, Turkey. E-mail: mkaracan@gazi.edu.tr; Fax: +90 312 2122279; Tel: +90 312 2021128*
[b]*Ahi Evran University, Science Faculty, Chemistry Department, Kirsehir, Turkey*

Experimental

Reagents and solutions

Glutathione Reductase (GR) from baker's yeast (*S. cerevisiae*) and other chemicals (GSSG, GSH, NADPH, NaH_2PO_4, Na_2HPO_4, and DMSO) were purchased from Sigma-Aldrich (USA). All chemicals were of HPLC reagent grade and used without additional purification. All solutions were prepared with ultrapure water. Glutathione reductase stock solution was prepared by dissolving 500 units of GR in 50 mL of phosphate buffer (0.02 M, pH 7.2) and stored at 4 °C. Stock solutions of 0.01 mol L^{-1} Sb(III) complexes were freshly prepared by dissolving each in a minimum amount of DMSO and diluting with water to a volume of 10 mL. Antimony complexes (Fig. 1) were synthesized according to procedures reported elsewhere.[42]

Apparatus

All voltammetric determinations were performed on a CHI 760d potentiostat. A three-electrode configuration with a hanging mercury drop electrode as the working electrode, Ag/AgCl electrode as the reference electrode, and a platinum wire as the auxiliary electrode were employed. A carbon ultramicro disc electrode (10 μm in diameter) was used in the chronoamperometric measurements as a working electrode. A standard one-compartment three-electrode cell with a volume of 10 mL (CGME cell and other electrodes were purchased from BAS Co., Ltd) was used in all electrochemical research. Ultrapure water (18.3 MΩ × cm resistivity) was obtained from a Milli-Q purification system (Merck, KGaA, Darmstadt, Germany). An Orion 5-Star Benchtop Multimeter was used for pH measurements (Thermo Fisher Scientific Inc., US). Prior to analysis, a solution was purged with high purity N_2 gas (99.999%) for about 10 min to remove oxygen.

Measurement of GR activity

The assay mixture (total volume, 10 mL) was prepared with 0.5 U of GR, 0.05 μmole NADPH and 0.02 M phosphate buffer (pH 7.2). After 2 min, the reaction was initiated by addition of 0.01 μmole of GSSG to the assay mixture. Inhibition of GR was studied in the presence of varying concentrations of Sb(III) compounds which were added to the mixture before GSSG.

Square wave voltammograms were recorded at 25 mV s^{-1} scan rate in the potential range of 0.0 to (−1.8) V (*vs.* Ag/AgCl) at every 20 s for 3 min. The degree of inhibition (as % activity) was calculated as the relative decrease of the GSH reduction peak current using the formula:[43]

$$\% \text{ activity} = 100 - I\%$$

$$I\% = [(i_0 - i_1)/i_0] \times 100$$

$$\% \text{ activity} = 100 - [(i_0 - i_1)/i_0] \times 100$$

where $I\%$ is the degree of inhibition, i_o is the steady-state current obtained in the absence of the inhibitor, and i_1 is the steady-state current obtained in the presence of the inhibitor. A steady-state response was obtained after 60 s. The percent activity values were determined by using peak currents obtained without and with the inhibitor (the last equation above). These values were plotted against inhibitor concentrations and the

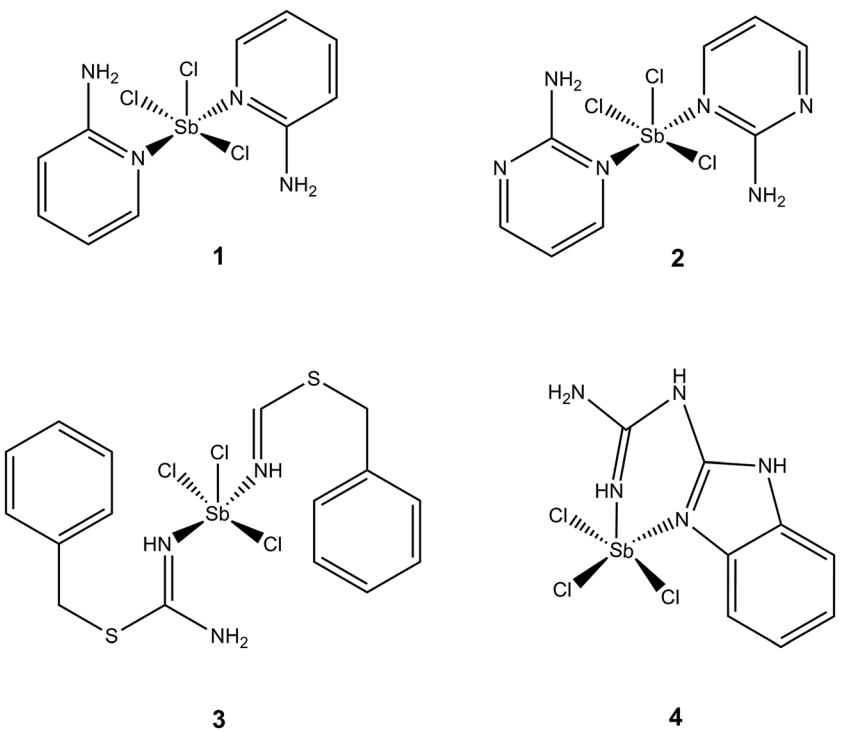

Fig. 1 Chemical structure of the antimony(III) complexes used in this study.

IC_{50} values were found thereof (Fig. 5). Each experiment was performed in triplicate at five different inhibitor concentrations with a constant GSSG concentration.

Electrochemical properties of the complexes

All voltammetric measurements were performed at room temperature and in aqueous media. Phosphate buffer (0.02 M, pH 7.2) was used as a supporting electrolyte. Diffusion coefficients and number of electrons transferred was found from the chronoamperometric Cottrell slopes of the 1 mM Sb(III) compounds with 1 mM ferrocene as the standard (a reversible transfer of 1 electron) on a C ultramicro disc electrode. Baransky equations were used to calculate the number of electrons transferred and the diffusion coefficients.[45]

Results and discussion

Optimization of GSH diffusion current measurement

Optimized working parameters of SWV with a hanging mercury drop electrode *versus* an Ag/AgCl electrode are given in Table 1.

The SW voltammograms recorded at increasing GSH concentrations in phosphate buffer (pH 7.2) are given in Fig. 2.

Reduction peak potential of GSH at optimized conditions was found at −0.44 V (*vs.* Ag/AgCl). This peak potential is slightly different from those reported in previous studies.[39,44] The differences may be due to the use of different electrodes and experimental conditions. Mladenov *et al.* report that the electrochemical activity of thiol-including substances at the mercury electrode is chiefly caused by biochemical interactions of the thiol with the electrode material.[44] They assert that upon anodic polarization of the electrode, an insoluble complex of GSH forms and is deposited onto the electrode surface. With a cathodic potential scan, the complex was reduced and the electrode reaction was given as follows:[44]

$$Hg(GS)_2 + 2e^- + 2H^+(aq) \rightarrow Hg(l) + 2GSH$$

Analytical characteristics of the SWV method for GSH are given in Table 2. The calibration graphs of the peak current *versus* GSH concentration were found to be linear in the range of 2.63–800 μM. The limit of detection (LOD) and the limit of quantitation (LOQ) were calculated as follows: LOD = $3s/m$, LOQ = $10s/m$; (m is the slope of the calibration line and s is the

Table 1 Optimized working parameters for SWV

Parameters	Value
Initial potential	0.0 V
Final potential	−1.8 V
Current range	10 μA
Frequency	10 Hz
Resting time	2 s
Pulse amplitude	25 mV
Purge time	30 s

Table 2 Analytical characteristics of the SWV method for GSH

Parameters	Value
Reduction potential	−0.44 V (*vs.* Ag/AgCl)
Range of linearity	2.63–800 μM
Calibration graph slope	0.0046 (A/M)
Correlation coefficient (R^2)	0.998
Blank standard deviation	1.21×10^{-3} μA
Limit of quantification (LOQ)	2.63 μM
Limit of detection (LOD)	0.79 μM
Relative error	2.5
Methods RSD ($N = 5$)	8.8

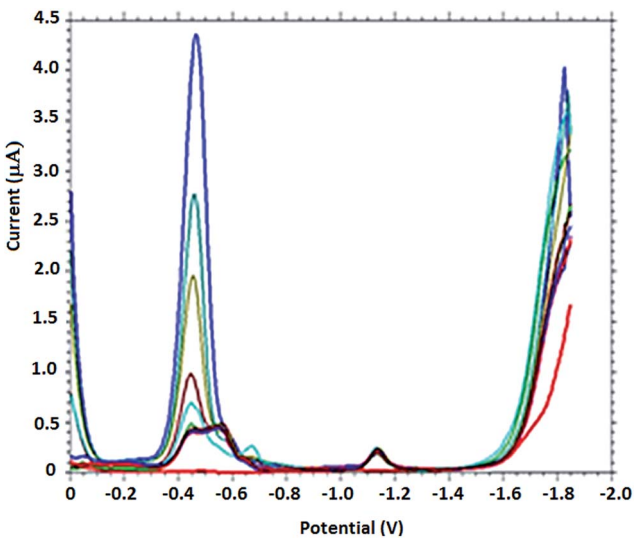

Fig. 2 SW voltammograms of GSH with increasing concentration in phosphate buffer (0.02 M, pH 7.2). Top to bottom curves: 12×10^{-4}, 5×10^{-4}, 3×10^{-4}, 1×10^{-4} mole L^{-1}.

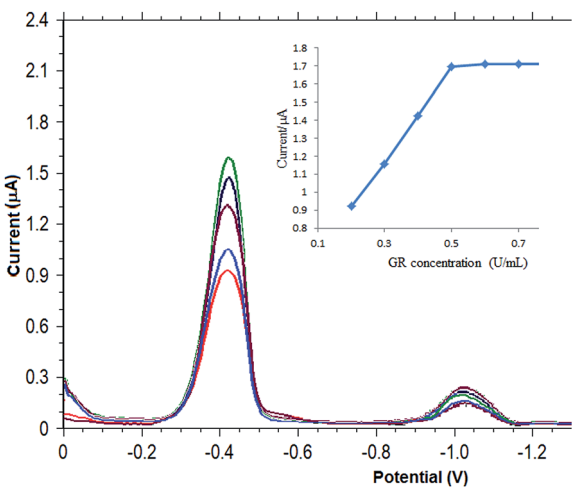

Fig. 3 GSH square wave voltammograms of consisting of increased enzyme concentrations in pH: 7.2, at HMDE, *vs.* Ag/AgCl and (inset) GSH current–GR concentration curve.

standard deviation of the current of the blank solution with $N = 10$).

The precision of the method was checked by taking 5 replicate measurements of GSH. Accuracy was checked by estimating the relative error between measured values after adding known concentrations.

Table 3 Optimized study conditions for GR activity

Parameters	Optimized value
Substrate concentration (GSSG)	1 μM
Substrate concentration (NADPH)	2 μM
Enzyme units	0.5 U
Enzymatic reaction time	60 s
pH	7.2

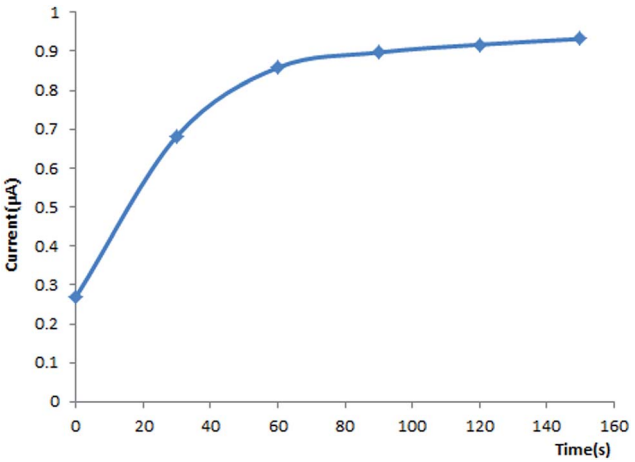

Fig. 4 Current–time graph of enzyme reaction in the presence of 0.5 U mL^{-1} GR.

Determination of GR activity

Activity of GR was evaluated by monitoring the production rate of GSH with SW voltammetry. SW voltammograms of enzymatic reactions were recorded at a 50 mV s^{-1} scan rate in the potential range of 0.0 to (−1.8) V with increasing enzyme concentration from 0.2 U mL^{-1} to 1.0 U mL^{-1} (Fig. 3). As the enzyme reaction proceeds, the concentration of GSH increases and the result is an increase in the peak current. Obviously, the increasing current of GSH for a given period is directly proportional to the GR enzymatic reaction rate; therefore it can be used to probe the glutathione reductase activity. Optimized working conditions of the enzymatic reaction are listed in Table 3.

Peak currents of GSH (inset of Fig. 3) reach a stable state at 0.5 U mL^{-1} of GR concentration. At the 0.5 U mL^{-1} GR concentration, the current of GSH shows a gradual increase up to 60 s, after that a plateau is reached, then there is no significant change in the current (Fig. 4). These optimized parameters were employed in later investigations of antimony(III) compounds.

Determination of IC_{50} values of the antimony(III) compounds

IC_{50} values were obtained from percent activity *versus* inhibitor concentration plots (Fig. 5). The data are shown in Table 4. In our previous study, we determined the IC_{50} values of the same compounds with a spectrochemical method by measuring the absorbances at 340 nm. IC_{50} values so obtained are also given in Table 4. It is apparent that the voltammetric IC_{50} values and their standard deviations are slightly better than the UV-based data. We attribute the difference to relatively better sensitivity of the voltammetric method. Interferences in spectrophotometric analysis are likely to cause an increase in the UV absorbance.

RSD values of the IC_{50} obtained by this voltammetric method are smaller than those relating to the UV absorption method.

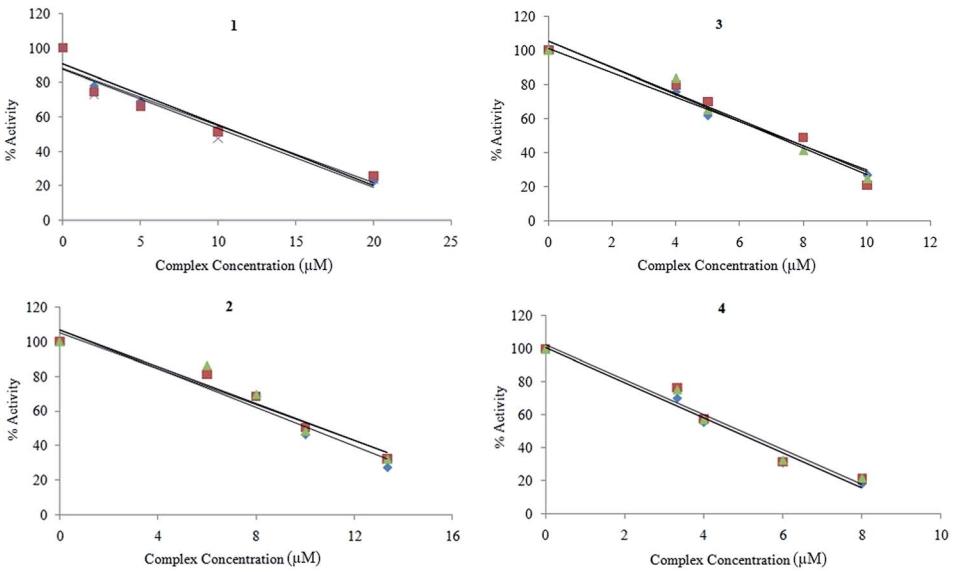

Fig. 5 % Activity–concentration graphs of the compounds in the presence of three different GSSG concentrations.

Table 4 IC_{50} and K_i values and of the antimony(III) compounds

Compounds	IC_{50} (μM) (with SWV)	RSD	IC_{50} (μM) (with UV[a])	RSD	K_i (μM) (with SWV)
1	11.65 ± 0.08	0.68	14.10 ± 0.13	0.92	2.60 ± 0.46
2	10.82 ± 0.13	1.2	12.10 ± 0.22	1.8	2.04 ± 0.31
3	7.34 ± 0.12	1.6	10.50 ± 0.21	2	1.56 ± 0.18
4	4.81 ± 0.18	3.7	5.37 ± 0.28	5.2	1.09 ± 0.08

[a] Taken from our previous study.[42]

The type of inhibition mechanism was assessed by plotting $1/V$ *versus* 1/[S] (Lineweaver–Burk[46] plot) with four different GSSG concentrations at constant NADPH concentration (Fig. 6), and initial velocity data was analyzed. It is seen that compounds act as a competitive inhibitor with respect to GSSG. Binding affinities of the inhibitors (K_i values) were also calculated from Lineweaver–Burk plots and equation of $K_i = \frac{IC_{50}}{1 + \frac{S}{K_m}}$ (Table 4).

Electrochemical properties of antimony(III) compounds

Cyclic voltammetric analyses of the antimony(III) compounds were performed in a mixture containing 100 μL of stock solution and 10 mL phosphate buffer (0.02 M, pH 7.2) at various scan rates (10, 50, 100, 500, 1000 mV s^{-1}) in the potential range 0.0 V to (−1.65) V (*vs.* Ag/AgCl), under a nitrogen atmosphere. Cyclic voltammograms are depicted in Fig. 7. Electrochemical data of the compounds are summarized in Table 5. Since the cathodic and anodic peaks are asymmetrical (peak separation is large) and the ratios of reverse to forward peak currents (i_a/i_c) range between 1.8 and 3.2 (at the scan rate at 0.05 V s^{-1}), the reduction observed is likely to reflect the Sb(III) in the complexes to Sb (0). Sb(III) in the complexes reduced at −0.345 V, −0.336 V, −0.332 V, and −0.278 V respectively at pH: 7.2, these values are consistent with literature.[47]

Linearity in the plot of $i_p - t^{-1/2}$ indicates that current is "diffusion controlled". In addition, the decreasing slope in the plot of $i_{pc}/v^{1/2}$ *versus* scan rate indicates the EC (electrochemical and chemical) mechanism (Fig. 8). The potential $E_{p/2}$ (half peak potential of the complex) varies with the nature of the ligands in the following order: **1** > **2** > **3** > **4** (Table 5). Comparison of this order with the GR inhibition activity series indicates that potential $E_{p/2}$ is directly proportional to the inhibition activity. According to Table 4, inhibitory activity of the compounds increases as follows: 1 < 2 < 3 < 4. Based on this series we inferred that (a) more N donor atom on an aromatic ring increases the activity and, (b) the

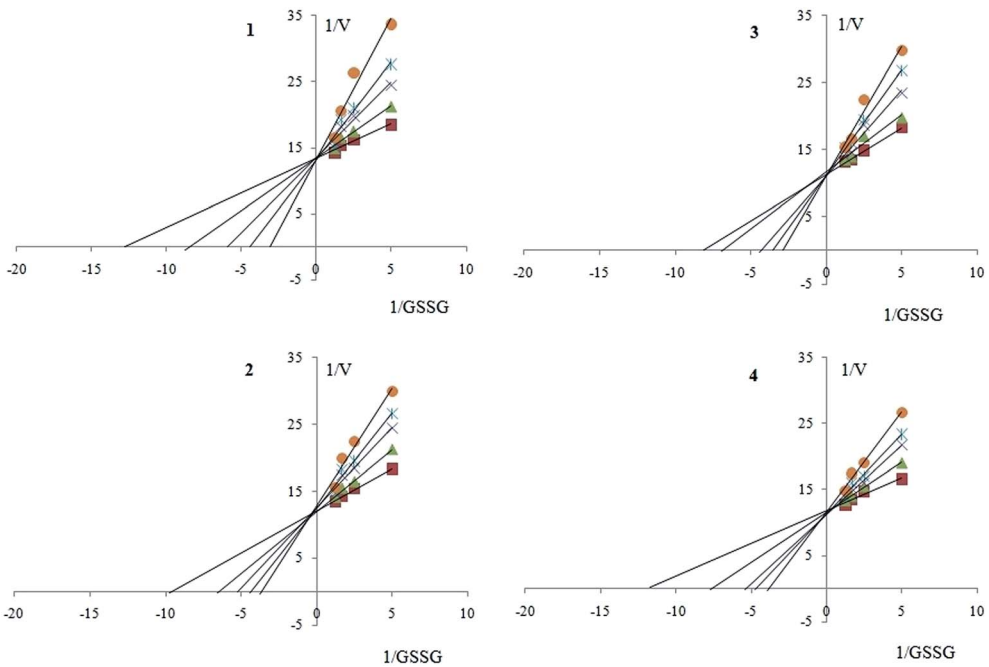

Fig. 6 Lineweaver–Burk plots of GR activity against varying GSSG concentrations.

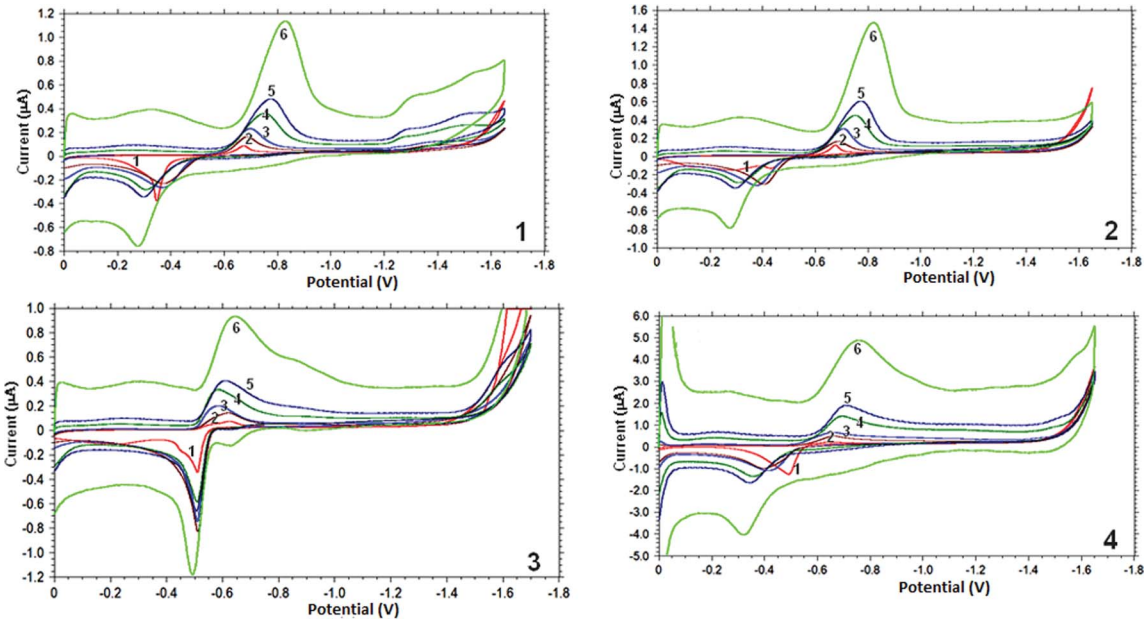

Fig. 7 Cyclic voltammograms of the compounds at different scan rates (**1**: 0.01; **2**: 0.05; **3**: 0.1; **4**: 0.5; **5**: 1; **6**: 5 v/s) in the phosphate buffer (0.02 M, pH 7.2).

Table 5 Some electrochemical data of the antimony(III) compounds

	1	**2**	**3**	**4**
$E_{pc} - E_{pa}$ (mV)	333	281	266	47
$E_{p/2}$ (V) (*vs.* Ag/AgCl)	−0.345	−0.336	−0.332	−0.278
i_{pa}/i_{pc}	1.864	1.406	2.825	3.240
Cottrell slope (S)	9.03×10^{-7}	8.33×10^{-7}	3.87×10^{-7}	7.65×10^{-7}
Limiting current (A)	3.47×10^{-10}	2.58×10^{-10}	5.88×10^{-11}	2.20×10^{-10}
Diffusion coefficient (D, $m^2\ s^{-1}$)	5.14×10^{-5}	3.34×10^{-5}	8.05×10^{-6}	2.88×10^{-5}
Transferred electron number	2.68	3.06	2.90	3.03

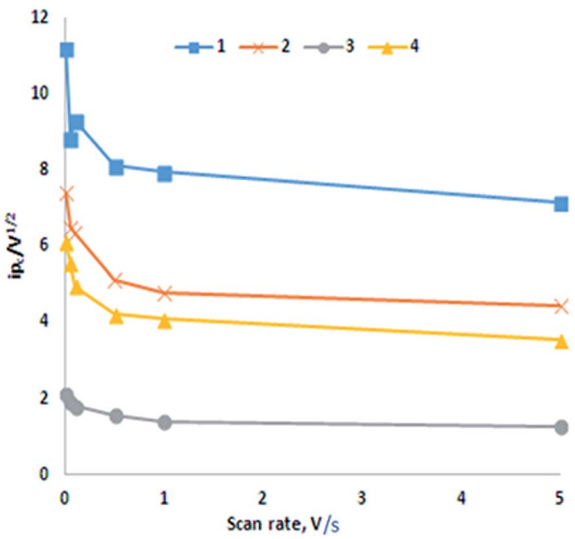

Fig. 8 Plot of the $i_{pc}/v^{1/2}$ *versus* scan rate.

guanidinobenzimidazole group has more activity than 2-benzyl-2-thiopseudeourea.

Compound **4**, the best inhibitor (Table 4), has the least negative potentials; that is, the easiest to reduce (Tables 4 and 5).

Conclusions

In this paper, we reported a comparatively simple procedure for measuring GR activity and screening GR inhibitors *in vitro*. This method is based primarily on the fact that the amount of GSH was directly detected using SWV. Working parameters for determining GR inhibitory activity were optimized with a hanging mercury drop electrode *versus* an Ag/AgCl electrode. IC_{50} values of four antimony(III) complexes were determined and compared with spectroscopic values. Obtained data showed that $E_{p/2}$ potentials of the compounds are directly proportional to GR inhibitory activity. Best inhibitors gain electrons to reduce easily.

RSD values of the data obtained by this proposed voltammetric method are smaller than those relating to UV absorption measurements.

Acknowledgements

This work has been supported in part by The Scientific and Technological Research Council of Turkey (TUBITAK) Project no: 212T089 and by Russian Foundation for Basic Research.

References

1 R. H. Schirmer, J. G. Müller and R. L. Krauth-Siegel, *Angew. Chem., Int. Ed.*, 1995, **34**, 141–154.
2 R. L. Krauth-Siegel, H. Bauer and R. H. Schirmer, *Angew. Chem., Int. Ed.*, 2005, **44**, 690–715.
3 S. Biswas, A. S. Chida and I. Rahman, *Biochem. Pharmacol.*, 2006, **71**, 551–564.
4 S. M. Kanzok, R. H. Schirmer, I. Turbachova, R. Iozef and K. Becker, *J. Biol. Chem.*, 2000, **275**, 40180–40186.
5 J. L. Rendon, I. P. Arenal, A. G. Flores, A. Uribe, A. Plancarte and G. M. Hernandez, *Mol. Biochem. Parasitol.*, 2004, **133**, 61–69.
6 A. Pastore, G. Federici, E. Bertini and F. Piemonte, *Clin. Chim. Acta*, 2003, **333**, 19–39.
7 J. Navarro, E. Obrador, J. Carretero, I. Petschen, J. Avino, P. Perez and J. M. Estrela, *Free Radical Biol. Med.*, 1999, **26**, 410–418.
8 D. M. Townsend, V. J. Findlay, F. Fazilev, M. Ogle, J. Fraser, J. E. Saavedra, X. Ji, L. K. Keefer and K. D. Tew, *Mol. Pharmacol.*, 2006, **69**, 501–508.
9 J. M. Estrela, A. Ortega and E. Obrador, *Crit. Rev. Clin. Lab. Sci.*, 2006, **43**, 143–181.
10 M. Kemp, Y. M. Go and D. P. Jones, *Free Radical Biol. Med.*, 2008, **44**, 921–937.
11 C. Perricone, C. De Carolis and R. Perricone, *Autoimmun. Rev.*, 2009, **8**, 697–701.
12 E. Dursun, M. Timur, B. Dursun, G. Suleymanlar and T. Ozben, *Journal of Diabetes and its Complications*, 2005, **19**, 142–146.
13 L. Cesaratto, C. Vascotto, C. D'Ambrosio, A. Scaloni, U. Baccarani, I. Paron, G. Damante, S. Calligaris, F. Quadrifoglio, C. Tiribelli and G. Tell, *Free Radical Res.*, 2005, **39**, 255–268.
14 M. Valko, C. J. Rhodes, J. Moncol, M. Izakovic and M. Mazur, *Chem.-Biol. Interact.*, 2006, **160**, 1–40.
15 S. Müller, T. W. Gilberger, Z. Krnajski, K. Lüersen, S. Meierjohann and R. D. Walter, *Protoplasma*, 2001, **217**, 43–49.
16 H. Ginsburg, O. Famin, J. Zhang and M. Krugliak, *Biochem. Pharmacol.*, 1998, **56**, 1305–1319.
17 O. Famin, M. Krugliak and H. Ginsburg, *Biochem. Pharmacol.*, 1999, **58**, 59–68.
18 V. L. Dubois, D. F. N. Platel, G. Pauly and J. Tribouley-Duret, *Exp. Parasitol.*, 1995, **81**, 117–124.
19 P. Srivastava, S. K. Puri, K. K. Kamboj and V. C. Pandey, *Trop. Med. Int. Health*, 1999, **4**, 251–254.
20 C. Biot, H. Bauer, R. H. Schirmer and E. Davioud-Charvet, *J. Med. Chem.*, 2004, **47**, 5972–5983.
21 I. Carlberg and B. Mannervik, *Methods Enzymol.*, 1985, **113**, 484–490.
22 T. Ohkuwa, Y. Sato and M. Naoi, *J. Chromatogr. B: Biomed. Sci. Appl.*, 1998, **705**, 23–28.
23 A. M. Piggott and P. Karuso, *Anal. Chem.*, 2007, **79**, 8769–8773.
24 A. A. Alves, L. Pereira da Silva, D. V. Macedo and L. T. Kubota, *Anal. Biochem.*, 2003, **323**, 33–38.
25 L. Yi, H. Li, L. Sun, L. Liu, C. Zhang and Z. Xi, *Angew. Chem., Int. Ed.*, 2009, **48**, 4034–4037.
26 G. Garai-Ibabe, L. Saa and V. Pavlov, *Anal. Chem.*, 2013, **85**, 5542–5546.
27 T. Santa, *Drug Discoveries Ther.*, 2013, **7**, 172–177.
28 E. Camera and M. Picardo, *J. Chromatogr. B: Anal. Technol. Biomed. Life Sci.*, 2002, **781**, 181–206.
29 J. P. Steghens, F. Flourie, K. Arab and C. Collombel, *J. Chromatogr. B: Anal. Technol. Biomed. Life Sci.*, 2003, **798**, 343–349.
30 K. Z. Constantinos, D. T. Paraskevas, D. K. Theano and G. T. Demetrius, *Anal. Chim. Acta*, 2013, **795**, 75–81.
31 R. R. Alvarez, L. E. Hernandez, J. Abadia and A. A. Fernandez, *Anal. Biochem.*, 2006, **356**, 254–264.
32 G. Hermann, K. Kryeziu and W. Berger, *Anal. Methods*, 2014, **2**, 3086–3094.
33 J. Reinbold, P. Koehler and M. Rychlik, *Anal. Biochem.*, 2014, **445**, 41–48.
34 Y. Ji, Y. Ma and X. Sun, *Anal. Methods*, 2013, **5**, 1542–1547.
35 G. Chwatko, E. Kuzniak, P. Kubalczyk, K. Borowczyk, M. Wyszczelska-Rokiela and R. Głowacki, *Anal. Methods*, 2014, **6**, 8039–8044.
36 B. K. McMahon and T. Gunnlaugsson, *J. Am. Chem. Soc.*, 2012, **134**, 10725–10728.
37 J. B. Raoof, R. Ojani, H. Karimi-Maleh, M. R. Hajmohamadi and P. Biparva, *Anal. Methods*, 2011, **3**, 2637–2643.
38 M. V. Corrêa-da-Silva, A. A. Pigoso, B. F. Ribeiro, L. O. Barbosa, C. A. Rosado Miloch and A. A. Alves, *Biosens. Bioelectron.*, 2013, **4**, 1–6.
39 B. Q. Yuan, X. Zeng, D. Deng, C. Xu, L. Liu, J. Zhang, Y. Gaoa and H. Pang, *Anal. Methods*, 2013, **5**, 1779–1783.
40 B. Q. Yuan, R. Zhang, X. Jiao, J. Li, H. Shi and D. Zhang, *Electrochem. Commun.*, 2014, **40**, 92–95.
41 B. Q. Yuan, X. Zeng, C. Xu, L. Liu, Y. Ma, D. Zhang and Y. Fan, *Sens. Actuators, B*, 2013, **184**, 15–20.
42 T. Tunc, Y. Koc, L. Açik, M. S. Karacan and N. Karacan, *Spectrochimica Acta Part (A)*, 2015, **136**, 1418–1427.
43 E. Wilkins, M. Carter, J. Voss and D. Ivnitski, *Electrochem. Commun.*, 2000, **2**, 786–790.
44 M. Mladenov, V. Mirceski, I. Gjorgoski and B. Jordanoski, *Bioelectrochemistry*, 2004, **65**, 69–76.
45 A. S. Baranski, W. R. Fawcett and C. M. Gilbert, *Anal. Chem.*, 1985, **57**, 166–170.
46 H. Lineweaver and D. Burk, *J. Am. Chem. Soc.*, 1934, **56**, 658–666.
47 M. S. El-Shahawi, A. S. Bashammakh, A. A. Al-Sibaai, S. O. Bahaffi and A. E. H. Al-Gohani, *Electroanalysis*, 2011, **23**(3), 747–754.

